Uncertainty in a Path-averaged Measurement of the Friction Velocity u_*

EDGAR L ANDREAS

U.S. Army Cold Regions Research and Engineering Laboratory, Hanover, New Hampshire

(Manuscript received 2 January 1992, in final form 13 April 1992)

ABSTRACT

Several electro-optical methods exist for measuring a path-averaged value of the inner scale of turbulence l_0. By virtue of Monin–Obukhov similarity, in the atmospheric surface layer such l_0 measurements are related to the friction velocity u_* or to the surface stress $\tau = \rho u_*^2$, where ρ is the air density. Because l_0 is a path-averaged quantity, u_* is too. Here the question of how precisely u_* can be measured is investigated by combining these inner-scale measurements with two-wavelength scintillation measurements that yield the sensible and latent heat fluxes and, thereby, facilitate stability corrections. The analysis suggests that current path-averaging instruments can generally measure u_* to ±20%–30%.

1. Introduction

The structure function of an atmospheric scalar—temperature, for example—is

$$D_t(r) = \overline{[t(\mathbf{x}) - t(\mathbf{x} + \mathbf{r})]^2}. \quad (1.1)$$

Here, t is the turbulent fluctuation in temperature, $\mathbf{x}$ and $\mathbf{x} + \mathbf{r}$ are two points in space, r is the magnitude of the vector $\mathbf{r}$, and the overbar indicates averaging. For large r values in the inertial subrange $D_t(r)$ is proportional to $r^{2/3}$; for small r values characterizing the turbulence dissipation region $D_t(r)$ is proportional to r^2. The inner scale of turbulence l_0 denotes the r value at which these two asymptotic forms are equal (Tatarski 1961, p. 46; Ishimaru 1978, p. 535). Hill and Clifford (1978) showed that

$$l_0 = [9\Gamma(1/3)\beta D]^{3/4}\epsilon^{-1/4}. \quad (1.2)$$

Here Γ is the gamma function of the indicated argument; β is the one-dimensional Kolmogorov constant,[1] which is roughly 0.4 (Andreas 1987); D is the thermal diffusivity of air; and ϵ is the dissipation rate of turbulent kinetic energy.

In the early 1970s, Strohbehn (1970), Gray and Waterman (1970), and Livingston (1972) discussed how optical propagation measurements in the atmosphere depend on l_0 and thereby suggested the possibility of measuring path-averaged values of l_0 electro-optically. The last decade has seen a flurry of papers that have demonstrated the practicality of such propagation measurements of l_0 (Hill and Ochs 1978; Ochs and Hill 1985; Ben-Yosef et al. 1986; Azoulay et al. 1988; Frehlich 1988; Thiermann and Azoulay 1989; Hill et al. 1992; Thiermann and Grassl 1992).

Because l_0 is the divide between two classes of propagation statistics, it is an important parameter for optical scientists studying atmospheric propagation. But, by virtue of (1.2), l_0 is also an important parameter for boundary-layer meteorologists; (1.2) shows that a measurement of l_0, in effect, is a measurement of ϵ, a key turbulence statistic. In turn, ϵ is directly related to the friction velocity u_*—the fundamental turbulence velocity scale in the atmospheric surface layer—by (Wyngaard and Côté 1971)

$$\epsilon = \left(\frac{u_*^3}{kz}\right)\phi_\epsilon(\zeta). \quad (1.3)$$

Here, k (=0.4) is the von Kármán constant; z is the measurement or path height; and $\phi_\epsilon(\zeta)$ is an empirical function of atmospheric stability, parameterized as $\zeta \equiv z/L$, where L is the Obukhov length,

$$\zeta = \frac{z}{L} = \frac{zgk}{u_*^2 T}\left(t_* + \frac{0.61T}{\rho + 0.61Q}q_*\right). \quad (1.4)$$

In (1.4), g is the acceleration of gravity; T is the average temperature; Q is the average absolute humidity; ρ is the density of moist air; and u_*, t_*, and q_* are turbulent flux scales. If τ is the momentum flux or surface stress, and H_s and H_L are, respectively, the sensible and latent heat fluxes,

$$\tau \equiv -\rho\overline{uw} \equiv \rho u_*^2, \quad (1.5)$$

$$H_s \equiv \rho c_p\overline{wt} \equiv -\rho c_p u_* t_*, \quad (1.6)$$

$$H_L \equiv L_v\overline{wq} \equiv -L_v u_* q_*. \quad (1.7)$$

[1] Hill and Clifford (1978) used the three-dimensional Kolmogorov constant in their Eq. (7); thus, (1.2) is different from their result by a factor of $(3/5)^{3/4}$.

Corresponding author address: Dr. Edgar L Andreas, Cold Regions Research and Engineering Laboratory, Department of the Army, Corps of Engineers, 72 Lyme Rd., Hanover, NH 03755-1290.

In these, u and w are turbulent fluctuations in the longitudinal and vertical velocity components, t and q are turbulent temperature and absolute-humidity fluctuations, c_p is the specific heat of air at constant pressure, and L_v is the latent heat of vaporization.

The fact that propagation measurements yield path-averaged values of l_0 and, thus, of ϵ and u_* is a benefit not lost on meteorologists. The need for areally averaged measurements of such quantities as the turbulent surface fluxes of momentum and sensible and latent heat is becoming more acute as meteorologists try, for example, to extrapolate in situ observations over areas that are the size of an airborne or satellite remote-sensor footprint.

Hill and Ochs (1983) anticipated the day when measuring values of all three meteorologically important surface fluxes in (1.5)–(1.7) would be possible. Andreas (1989, 1990b, 1991) has discussed using electro-optical propagation instruments—namely, scintillometers—to measure path-averaged values of the sensible and latent heat fluxes and has analyzed the theoretical uncertainties in these measurements. Hill et al. (1988, 1992) and Thiermann and Grassl (1992) have demonstrated these scintillation techniques for measuring heat fluxes. Using Wyngaard and Clifford's (1978) analysis of the errors in estimating momentum and heat fluxes from structure parameters, Hill (1982) evaluated the uncertainty in measuring l_0 electro-optically. Later, he looked at instrumental constraints on path-averaged measurements of l_0 (Hill 1988; Hill and Lataitis 1989). Moroni et al. (1990) used a Monte Carlo error analysis to update Wyngaard and Clifford's study. No one, however, has yet evaluated the precision with which u_* can be measured with a full path-averaging system that includes a long-wavelength scintillometer to account for the effects of the latent heat flux. That sensitivity analysis will be done here. The question is "How precisely can we measure ϵ and u_* by using path-averaging electro-optical propagation instruments to measure l_0, H_s, and H_L?"

2. Path-averaged fluxes

Figure 1 depicts the rudiments of the flux-measuring system that is considered here. Andreas (1989, 1990a,b, 1991) showed that it is theoretically possible to measure path-averaged values of the temperature structure parameter C_t^2 and the humidity structure parameter C_q^2 by using scintillometers (Wang et al. 1978) to measure the refractive-index structure parameter C_n^2 at short (λ_1) and long (λ_2) wavelengths. Hill et al. (1988) demonstrated this concept experimentally. A short wavelength is one in the visible, near-infrared, or midinfrared region of the electromagnetic (EM) spectrum; a long wavelength is in the millimeter or radio region.

By providing C_t^2 and C_q^2, the λ_1 and λ_2 scintillometers yield path-averaged values of the sensible and latent heat fluxes if we also know the velocity scale u_*. The third scintillation measurement in Fig. 1 helps provide

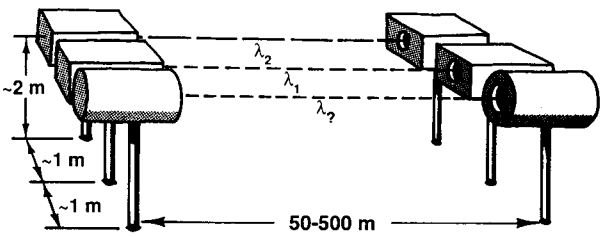

FIG. 1. Schematic of the scintillation instruments needed for path-averaged measurements of the turbulent fluxes of momentum and sensible and latent heat.

that. Hill (1988) reviewed three scintillation techniques for measuring l_0. Each of these involves scintillation measurements using two short EM wavelengths; in Fig. 1 these would be the λ_1 and $\lambda_?$ scintillometers. One method derives l_0 from the irradiance variances measured by two scintillometers that both operate at λ_1 (i.e., $\lambda_? = \lambda_1$) but differ by having large-diameter and small-diameter apertures (Hill and Ochs 1978; Ochs and Hill 1985; Hill et al. 1992). A second method finds l_0 from the irradiance variances for two spherical-wave scintillometers that both operate at short wavelengths, say λ_1 and $\lambda_? = \lambda_3$ (Azoulay et al. 1988). The third method obtains l_0 from the bichromatic correlation of two scintillating short waves, again λ_1 and $\lambda_? = \lambda_3$ (Ben-Yosef et al. 1986; Azoulay et al. 1988; Thiermann and Azoulay 1989; Thiermann and Grassl 1992). (For this third method, Fig. 1 is not quite accurate because beam splitters must be used to make the paths of the two waves coincident.)

In the subsequent analysis, the method for measuring l_0 is immaterial. Besides, Hill (1988) and Hill and Lataitis (1989) have already evaluated the uncertainty in the l_0 measurement for several potential methods. Here, it is simply assumed that we somehow measure l_0 electro-optically; our focus is on the precision of the ϵ and u_* values that can be obtained from these path-averaged propagation measurements. Andreas (1989, 1990a) has already evaluated the precision of such H_s and H_L measurements.

3. u_* sensitivity under neutral stability conditions

Because we are interested in finding ϵ from measurements of l_0, rewrite (1.2) as

$$\epsilon = [9\Gamma(1/3)\beta D]^3 l_0^{-4}. \quad (3.1)$$

From this, we see that differential changes in ϵ, l_0, β, and D must obey

$$d\epsilon = \left(\frac{\partial \epsilon}{\partial l_0}\right) dl_0 + \left(\frac{\partial \epsilon}{\partial \beta}\right) d\beta + \left(\frac{\partial \epsilon}{\partial D}\right) dD. \quad (3.2)$$

Evaluating the partial derivatives by using (3.1), we obtain

$$\frac{d\epsilon}{\epsilon} = -4\left(\frac{dl_0}{l_0}\right) + 3\left(\frac{d\beta}{\beta}\right) + 3\left(\frac{dD}{D}\right). \quad (3.3)$$

I interpret these ratios of differential changes to actual values as relative uncertainties. Thus, the relative uncertainty in an ϵ measurement that is based on an inner-scale measurement reflects the relative uncertainty in the l_0 measurement as well as uncertainties in the values of the molecular diffusivity and the scalar Kolmogorov constant. For example, if $dl_0/l_0 = \pm 10\%$, $d\beta/\beta = \pm 5\%$, and $dD/D = \pm 2\%$, then $d\epsilon/\epsilon = \pm 61\%$.

Under neutral stability conditions (i.e., $\zeta = 0$), $\phi_\epsilon(\zeta) = 1$ in (1.3); thus,

$$u_* = (\epsilon k z)^{1/3}. \tag{3.4}$$

On looking at differential changes in u_*, we see that

$$\frac{du_*}{u_*} = \frac{1}{3}\left(\frac{d\epsilon}{\epsilon}\right) + \frac{1}{3}\left(\frac{dz}{z}\right) + \frac{1}{3}\left(\frac{dk}{k}\right). \tag{3.5}$$

With (3.3), this becomes

$$\frac{du_*}{u_*} = -\frac{4}{3}\left(\frac{dl_0}{l_0}\right) + \frac{1}{3}\left(\frac{dz}{z}\right) + \frac{d\beta}{\beta} + \frac{dD}{D} + \frac{1}{3}\left(\frac{dk}{k}\right). \tag{3.6}$$

Thus, under neutral stability conditions, the relative uncertainty in the quantity of interest, u_*, is only 33% larger than the relative uncertainty in the primary observable, l_0. In other words, l_0 is a good predictor of u_*.

4. u_* sensitivity under nonneutral stability conditions

In the real atmospheric surface layer, the stability is rarely neutral. Thus, instead of (3.4), in the sensitivity analysis we must use (1.3). For $\phi_\epsilon(\zeta)$ here, the form originally given by Wyngaard and Côté (1971) is used but modified for a von Kármán constant of 0.4 rather than 0.35 (Andreas 1988b):

$$\phi_\epsilon(\zeta) = [1 + 0.46(-\zeta)^{2/3}]^{3/2} \quad \text{for} \quad -10 \leq \zeta \leq 0, \tag{4.1a}$$

$$= (1 + 2.3\zeta^{3/5})^{3/2} \quad \text{for} \quad 0 \leq \zeta \leq 2. \tag{4.1b}$$

Fairall et al. (1980) and Schacher et al. (1981) have corroborated these expressions for $-10 \leq \zeta \leq 2$.

From (1.3), we see that

$$d\epsilon = \left(\frac{\partial \epsilon}{\partial u_*}\right) du_* + \left(\frac{\partial \epsilon}{\partial z}\right) dz + \left(\frac{\partial \epsilon}{\partial \zeta}\right) d\zeta, \tag{4.2}$$

where here and henceforth uncertainties in constants such as k are ignored; such uncertainties cause systematic rather than random errors. Also, Wyngaard and Clifford (1978) and Moroni et al. (1990) have looked at how uncertainties in some of these constants affect flux measurements. In (4.2), ζ is a derived rather than a fundamental variable; hence, in (4.2) we must substitute [see (1.4)]

$$d\zeta = \left(\frac{\partial \zeta}{\partial z}\right) dz + \left(\frac{\partial \zeta}{\partial u_*}\right) du_* + \left(\frac{\partial \zeta}{\partial t_*}\right) dt_* + \left(\frac{\partial \zeta}{\partial q_*}\right) dq_*. \tag{4.3}$$

Consequently,

$$d\epsilon = \left(\frac{\partial \epsilon}{\partial u_*} + \frac{\partial \epsilon}{\partial \zeta}\frac{\partial \zeta}{\partial u_*}\right) du_* + \left(\frac{\partial \epsilon}{\partial z} + \frac{\partial \epsilon}{\partial \zeta}\frac{\partial \zeta}{\partial z}\right) dz + \left(\frac{\partial \epsilon}{\partial \zeta}\frac{\partial \zeta}{\partial t_*}\right) dt_* + \left(\frac{\partial \epsilon}{\partial \zeta}\frac{\partial \zeta}{\partial q_*}\right) dq_*. \tag{4.4}$$

What follows from (4.4) is routine calculus and algebra. Thus, this sensitivity analysis is finished in the Appendix and only the final sensitivity equation is reported here. This is

$$\frac{du_*}{u_*} = S_\epsilon\left(\frac{d\epsilon}{\epsilon}\right) + S_{zz}\left(\frac{dz}{z}\right) + S_{C_1}\left(\frac{dC_{n1}}{C_{n1}}\right) + S_{C_2}\left(\frac{dC_{n2}}{C_{n2}}\right). \tag{4.5}$$

As before, du_*/u_* is the relative uncertainty in the u_* measurement; and $d\epsilon/\epsilon$ is the relative uncertainty in the ϵ value obtained from the l_0 measurement. Therefore, (3.3) could have been substituted for $d\epsilon/\epsilon$ in (4.5); dz/z is the relative uncertainty in the path height. Because stability conditions are, in general, nonneutral, we must incorporate measurements of t_* and q_* from the λ_1 and λ_2 scintillometers (Fig. 1) into our analysis to make stability corrections. Consequently, the uncertainties in the refractive index structure parameters measured by the λ_1 and λ_2 scintillometers, which appear in the form dC_{n1}/C_{n1} and dC_{n2}/C_{n2} in this analysis, also affect the u_* measurement.

In (4.5), the S's are called sensitivity coefficients. These are analogous to the numerical coefficients in (3.3) or (3.6), for example, and, as such, show how uncertainties in the fundamental observables, ϵ (or l_0), z, C_{n1}^2, and C_{n2}^2, get mapped into an uncertainty in the derived quantity, u_*. The Appendix gives the functional forms of the S's. Here $S_\epsilon(\zeta)$ and $S_{zz}(\zeta)$ depend only on the stability. Coefficients $S_{C_1}(\zeta, \text{Bo}, \lambda_1, \lambda_2)$ and $S_{C_2}(\zeta, \text{Bo}, \lambda_1, \lambda_2)$ depend on the stability; on the Bowen ratio,

$$\text{Bo} = H_s/H_L; \tag{4.6}$$

on the two EM wavelengths, λ_1 and λ_2; and weakly on temperature, humidity, and barometric pressure.

Figure 2 shows the values of S_ϵ, S_{zz}, and $S_{l_0} = -4S_\epsilon$ [see (3.3)] for the range of stabilities over which (4.1) is valid. Hill (1982) suggested that the relative uncertainty in l_0 measurements could be about $\pm 3\%$; his recent review (1988) also implied that, with careful instrumental design, l_0 could be measured to within a few percent. Actual l_0 measurements (Hill and Ochs 1978; Ochs and Hill 1985; Azoulay et al., 1988; Thiermann and Azoulay 1989), however, show more variability—perhaps $\pm 10\%$. Using this larger uncertainty, (4.5) and Fig. 2 show that for $-2 \leq z/L \leq 0.5$ uncertainty in the path-averaged l_0 measurement contributes about $\pm 20\%$ to the uncertainty in u_*. If the techno-

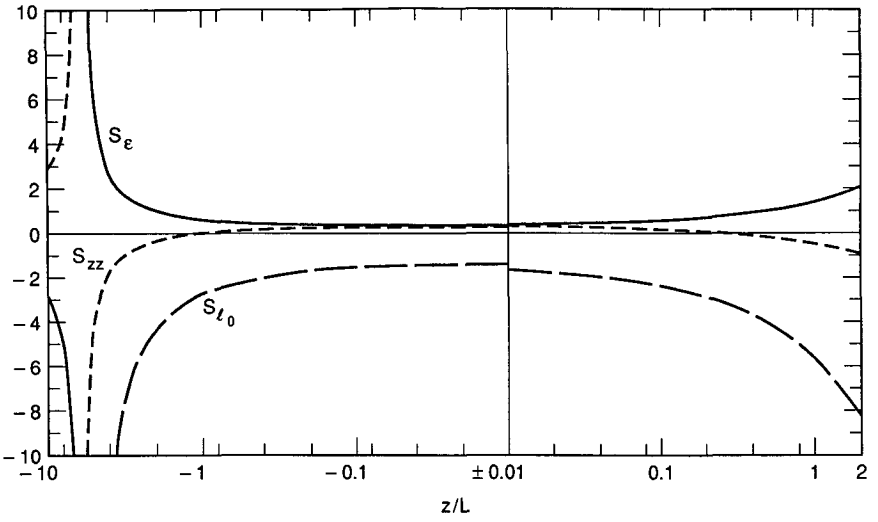

FIG. 2. The sensitivity coefficients S_ϵ, S_{zz} [see (4.5)], and S_{l_0} ($= -4S_\epsilon$) as functions of the stability z/L.

logical improvements that Hill (1988) identified as being crucial to the accuracy of l_0 measurements can be made, the theoretical uncertainty in the u_* measurement could be made less.

Uncertainty in the path or measurement height, dz/z, may depend more on the terrain than on our measurement capabilities. As an example of fairly smooth terrain, suppose $dz/z = \pm 2\%$. Then according to Fig. 2, the S_{zz} term in (4.5) would contribute $\pm 1\%$ or less to the uncertainty in u_* unless $z/L < -4$.

Notice, in Fig. 2, S_ϵ, S_{zz}, and S_{l_0} all get large in magnitude when z/L is near -6. Equations (A.17), (A.19), and (A.20) explain this behavior. Here $f(\zeta)$ approaches infinity, and S_ϵ, S_{l_0}, and S_{zz} thus have simple poles if $(\zeta/\phi_\epsilon)(\partial\phi_\epsilon/\partial\zeta)(S_{u_*} - 4)$ is ever near -3, which it is in the vicinity of $z/L = -6$. Here it would be impossible to find u_* with path-averaging instruments. We must interpret this conclusion with caution, however. The location of the poles in S_ϵ, S_{l_0}, and S_{zz}—in fact, the very existence of the poles—is quite sensitive to the behaviors of $\phi_\epsilon(\zeta)$ and $g(\zeta)$, the nondimensional profile of the refractive index structure parameter (Andreas 1989). The region where the poles occur, $z/L < -2$, is the free-convection region, where u_* begins to lose significance. In other words, the region where the path-averaging measurements break down is a meteorological regime in which any instrument would have difficulty measuring u_*. This is, in fact, why $\phi_\epsilon(\zeta)$ and $g(\zeta)$ are more uncertain in this region. In summary, although the poles in Fig. 2 are suggestive of the difficulties in measuring u_* when $-z/L$ is large, we should not put much confidence in the actual S_ϵ, S_{l_0}, and S_{zz} values when $z/L < -2$. Fortunately, here other path-averaging techniques exist for measuring the sensible and latent heat fluxes without the need for also measuring u_* (Andreas 1991).

The sensitivity coefficients S_{C_1} and S_{C_2} in (4.5) depend not only on ζ but also on λ_1, λ_2, and Bo. Previous analyses (Andreas 1989, 1990a, 1991) all demonstrated that optimizing the two-wavelength method for measuring heat fluxes requires pairing a short EM wavelength—one in the visible or infrared—with a long wavelength—one in the millimeter or radio region. Figures 3 and 4 show S_{C_1} and S_{C_2} for two practical two-wavelength pairs.

Both S_{C_1} and S_{C_2} suffer from the same pole that affects S_ϵ, S_{l_0}, and S_{zz} [see (A.21) and (A.22)]. Thus, when z/L is near -6, these coefficients also approach infinity. But for z/L values between -2 and 2, Figs. 3 and 4 show that $|S_{C_1}|$ and $|S_{C_2}|$ are generally 1 or less. Equations (3.5) or (A.21) and (A.22) show that both S_{C_1} and S_{C_2} must be uniformly zero when $\zeta = 0$. This is a fourth, implicit reference line in the figures. For $-2 \leqslant z/L \leqslant 2$, S_{C_1} and S_{C_2} always lie between zero and the $z/L = \pm 2$ lines plotted in Figs. 3 and 4.

Both S_{C_1} and S_{C_2} also have a simple pole and, thus, go to infinity when Bo $= -0.0714$ for these environmental conditions. Physically, at this pole the sensible and latent heat fluxes are both finite but nonzero, are in opposite directions, and have magnitudes that cancel each other's effect on the stability [see (A.1) or Andreas (1989, 1991)]. Thus ζ is zero, and both ζ_T/ζ and ζ_Q/ζ are infinite [see (A.21) and (A.22)]. Since the stability is neutral at the pole ($\zeta = 0$), (4.5) is not the proper equation to use in estimating the uncertainty in u_* right at the pole; (3.5) or (3.6) is more appropriate. The pole is very narrow, however. Small changes in Bo produce ζ values far from zero but still on curves in the vicinity of the pole that are associated with large magnitudes for S_{C_1} and S_{C_2}.

Fortunately, this pole is localized and in a Bowen-ratio region not often encountered over land. Most of the weak effects that temperature, humidity, and barometric pressure have on S_{C_1} and S_{C_2} for a given wave-

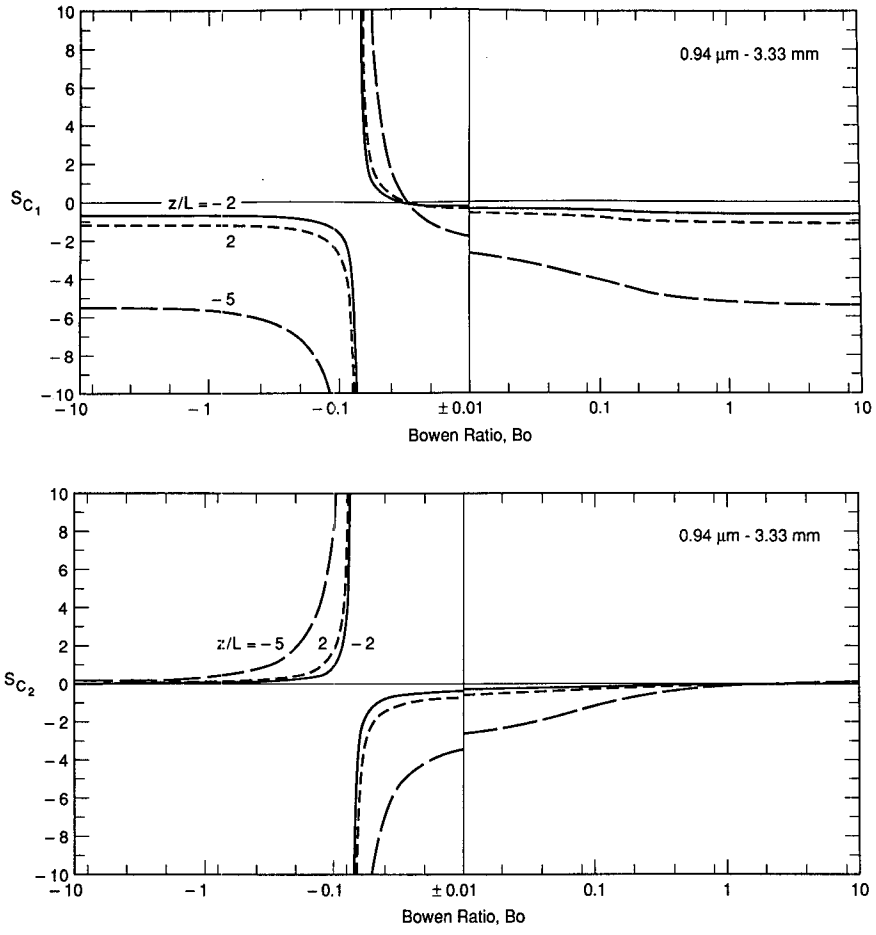

FIG. 3. The sensitivity coefficients S_{C_1} and S_{C_2} in (4.5) for the two-wavelength pair 0.94 μm and 3.33 mm (90 GHz) as functions of the Bowen ratio and for three stabilities. Environmental conditions are $T = 20°C$, $Q = 1.39$ kg m^{-3} (relative humidity of 80%), and a barometric pressure of 1000 hPa.

length pair come through their influence on the location of this pole. Andreas (1989, 1991) showed that as the temperature increases from −40° to 40°C the location of this pole moves only from −0.05 to −0.08, a range infrequently observed over land.

Under meteorological conditions that lead to Bowen ratios near −0.07 or to z/L values near −6, the uncertainty in the u_* measurement caused by uncertainties in C_{n1}^2 and C_{n2}^2 will be very large. But for Bo < -0.1 or Bo > 0 and for $-2 \leq z/L \leq 2$, Figs. 3 and 4 show that uncertainties in the C_{n1}^2 and C_{n2}^2 measurements contribute little to the uncertainty in u_*. Typically, C_n^2 can be measured to ±10%; therefore, in (4.5) dC_{n1}/C_{n1} and dC_{n2}/C_{n2} are both about ±5%. Away from the poles in Figs. 3 and 4, $|S_{C_1}|$ is typically 1 or less, and S_{C_2} is near 0. Hence, the S_{C_1} and S_{C_2} terms in (4.5) contribute only about ±5% to the uncertainty in the u_* measurement.

On summing the uncertainties estimated for the terms in (4.5), we find that, typically, $du_*/u_* \approx \pm 20\% \pm 1\% \pm 5\% \pm 0\% = \pm 26\%$. This experimental uncertainty is larger than the ±10% commonly ascribed to eddy-correlation measurements of u_*. But the advantage here is that these scintillation measurements average spatially and would, presumably, yield more representative u_* values than eddy-correlation measurements at a single point. Moreover, if the accuracy of the l_0 measurement can be reduced to the few percent that Hill (1982, 1988) feels is possible, these scintillation measurements of u_* would be nearly as accurate as eddy-correlation measurements.

As has been mentioned, the cornerstone of the two-wavelength scintillation measurements of sensible and latent heat is the pairing of short-wavelength and long-wavelength scintillometers. But such a pairing is not essential if we are interested *only* in u_* and H_s measurements. Figure 5 shows S_{C_1} and S_{C_2} for a two-wavelength combination that would be considered a poor choice for latent heat flux measurements (Andreas 1990a, 1991), 0.94 and 10.6 μm. Here, however, though the values of S_{C_1} and S_{C_2} are basically reversed from those in Figs. 3 and 4, the sum of their absolute values is not much larger than the sums in these figures. That is, uncertainty in the u_* measurement with the

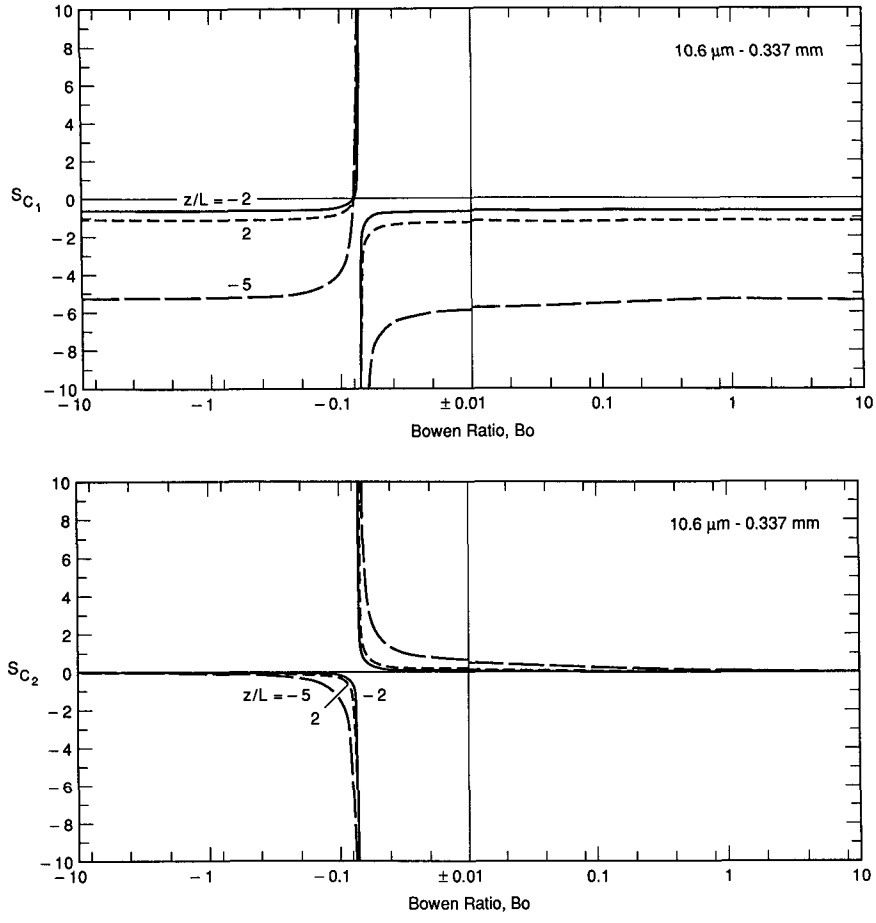

FIG. 4. As in Fig. 3 except this is the two-wavelength pair 10.6 μm and 0.337 mm (890 GHz).

0.94–10.6-μm pair would not be significantly worse than with the 0.94-μm–3.33-mm or 10.6-μm–0.337-mm pairs. The H_s measurement would also be adequate with the 0.94–10.6-μm pair, but measurements of H_L would be far worse than with the other two pairs (Andreas 1990a). Evidently, the 0.94–10.6-μm pair has enough water vapor discrimination to yield ζ values that are good enough for an accurate stability correction in the u_* measurements. Wavelengths closer together, such as 0.63 and 0.94 μm, do not have this ability to discriminate between scintillations caused by turbulent temperature and water vapor fluctuations and, thus, would contribute large uncertainties to a complete scintillation measurement of u_*.

Continuing along this line, we can imagine a variety of other sensor subsets that path average some but not all three of the fluxes. In free convection, for example, u_* becomes irrelevant; the sensible and latent heat fluxes can, thus, be obtained from measurements of C_{n1}^2 and C_{n2}^2 alone (Andreas 1991). Kohsiek and Herben (1983) even eliminated the C_{n1}^2 measurement and obtained the sensible and latent heat fluxes in free convection from a radio-wavelength measurement of C_{n2}^2 and presumed relationships between C_t^2, C_q^2, and C_{tq}, the temperature–humidity structure parameter. Hill et al. (1988) measured C_{n1}^2 and C_{n2}^2 over long paths but measured u_* with a nearby three-axis sonic anemometer. The heat fluxes they reported thus combined both point and path-averaged measurements. Recently, Thiermann and Grassl (1992) and Hill et al. (1992) reported measurements of u_* and H_s obtained from two short-wavelength scintillometers (λ_1 and $\lambda_?$) in dry conditions where H_L was negligible. This same sensor combination would surely yield useful measurements in conditions with nonnegligible H_L if it were complemented with a measurement of the Bowen ratio. With the Bowen ratio, we could account for the effects of the moisture flux on stability [see (A.1)] and could estimate H_L from the path-averaged H_s value [see (4.6)]. An uncertainty analysis for the u_* value obtained with this combination of sensors would again start with (4.2); but (4.3) would now have a Bo term instead of the q_* term.

5. Observational considerations

Intermittency confounds the measurement of microscale turbulence in the atmosphere. Because path-

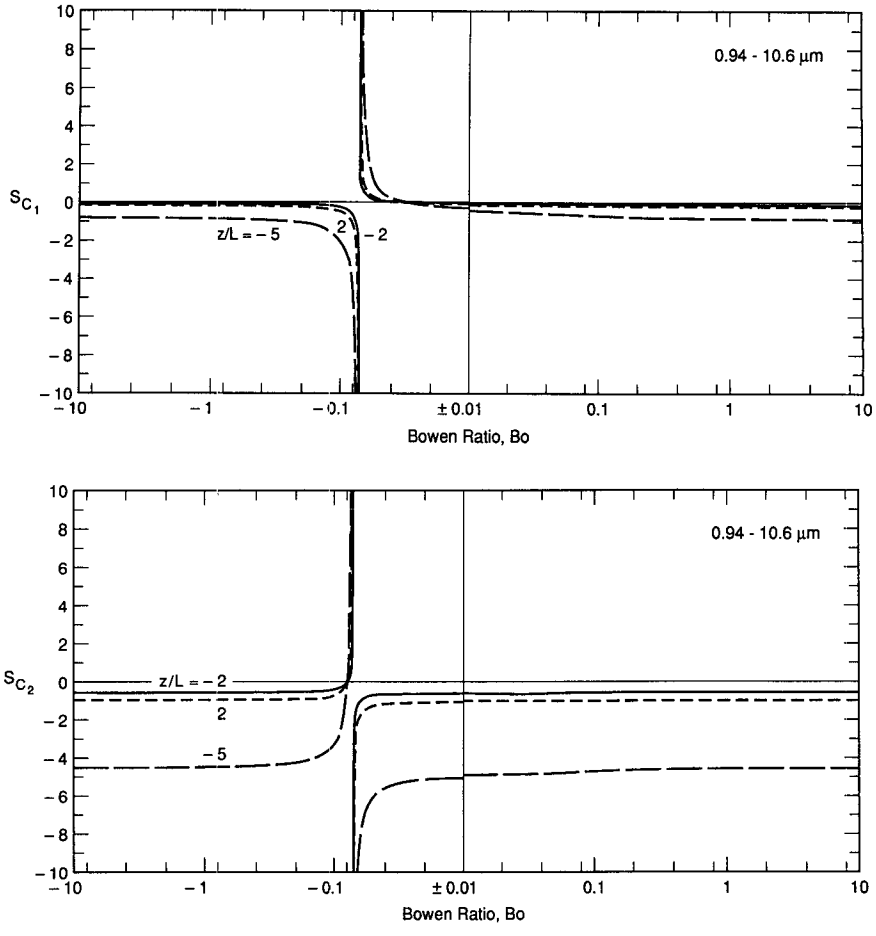

FIG. 5. As in Fig. 3 except this is the two-wavelength pair 0.94 and 10.6 μm.

averaging instruments can yield statistically stable estimates of l_0 and C_n^2 in a very short time—on the order of a few seconds (e.g., Frehlich 1988)—dealing with intermittency is especially important in interpreting measurements from such instruments. In this section, the following two questions are considered: 1) "Is (1.2) accurate in the presence of intermittency?" and 2) "How long must we average to obtain optimal estimates of the fluxes?"

The second question is the easier to answer and is, in fact, one that was considered in a previous study (Andreas 1988a). Haugen et al. (1971) and Wyngaard (1973) have shown that measuring the momentum and heat fluxes requires averaging for 30–60 min because of the longer time scales of the processes that contribute to these fluxes. A second consideration is that computing fluxes from the path-averaged measurements necessitates invoking Monin–Obukhov similarity. The similarity functions required were generally derived from measurements of u_*, t_*, q_*, ϵ, and the profiles of wind speed, temperature, and humidity that satisfied this requirement of averaging for 30–60 min. That these similarity functions are also valid for much shorter averaging times has not been demonstrated. Indeed, it is not clear that this is demonstrable. The fundamental time scale of a first moment in the atmospheric surface layer is the inverse of the strain rate (Tennekes and Lumley 1972, p. 65), z/u_*—which is tens of seconds. Sampling considerations suggest that measuring profiles accurately requires averaging for at least an order of magnitude longer than z/u_*—that is, for several hundred seconds. Therefore, we see that although it is possible to measure l_0 and C_n^2 with some statistical certainty in a very short time, estimating fluxes from these values via Monin–Obukhov similarity is not statistically, experimentally, or theoretically justified. To obtain surface-layer fluxes from path-averaging instruments, we must still follow the same guidelines that apply to point sensors: average for 30–60 min (Wyngaard 1973).

A fundamental answer to the first question posed—"Is (1.2) accurate?"—deserves theoretical and experimental studies beyond the scope of this paper. The question, in essence, is "What form does the instantaneous refractive index spectrum have in the inertial–convective and dissipation regions?" Following Tennekes and Lumley (1972, p. 260), it is estimated that the time required for a burst of turbulent energy to

cascade through the spectrum from its production region (associated with an outer scale of roughly z) to its dissipation region (scale length of l_0) is again roughly z/u_*. Remember, this scale is typically tens of seconds. Thus, just defining what we mean by an instantaneous spectrum is fairly tricky business. If the averaging time is too short, scales in the dissipation region will not reflect the energy being transferred through the inertial–convective subrange. Again, some of these averaging problems have been considered elsewhere (Andreas 1988a).

Operationally, however, the answer to the first question is straightforward. The preceding discussion of question 2 established that we must averaged for 30–60 min. Models of the scalar spectrum—on which (1.2) is based—were derived from such lengthy averages. Therefore, I am invoking (1.2) in precise accordance with its definition: The long averaging times smooth the effects of any intermittency.

6. Conclusions

Methods for measuring the turbulent surface fluxes of momentum, heat, and moisture over broad areas would perfectly complement the resolution, speed, and sophistication of current numerical mesoscale or climate models. The measuring technique discussed here—obtaining the momentum flux or, alternatively, u_* by electro-optically measuring the inner scale of turbulence, l_0—is one component of a system for measuring path-averaged values of these key surface fluxes.

The u_* sensitivity equation for nonneutral stability [(4.5)] shows how uncertainties in the measured fundamental variables, l_0 (or ϵ), z, C_{n1}^2, and C_{n2}^2, affect the accuracy of the desired variable u_*. The l_0 measurement contributes the largest uncertainty and is where we should concentrate our developmental efforts. The λ_1 and λ_2 scintillometer measurements that provide C_{n1}^2 and C_{n2}^2 (see Fig. 1) contribute only modest uncertainty to the u_* measurement but are, nevertheless, crucial components of this system: Combined with u_*, they yield the path-averaged sensible and latent heat fluxes.

In summary, the sensitivity analysis leads to the following conclusions.

1) Path-averaging methods for obtaining u_* and the latent heat fluxes have large uncertainties when the Bowen ratio Bo is in the vicinity of -0.07, which it rarely is over natural surfaces.

2) Path-averaging methods for obtaining u_* have large uncertainties when z/L is less than -2. This is the free-convection region, however, where u_* begins to lose significance and other path-averaging techniques exist for finding the heat fluxes (Andreas 1991).

3) For other conditions, with current path-averaging technology, u_* can theoretically be measured to ±20%–30%. This is roughly twice the uncertainty ascribed to eddy-correlation measurements of u_*. But these path-averaged u_* measurements have two advantages: (a) They are remote from the sampling instruments and thus undisturbed by them; and (b) they should be more representative because of the inherent spatial averaging.

4) Improving the precision of the l_0 measurements by incorporating Hill's (1988) suggestions, for example, into new instruments could make the path-averaging measurements nearly as precise as eddy-correlation measurements.

Acknowledgments. I would like to thank S. F. Ackley, M. J. Hardenberg, R. J. Hill, A. W. Hogan, W. Kohsiek, and V. Thiermann for reviewing the manuscript. The Department of the Army supported this research through Project 4A161102AT24.

APPENDIX

Derivation of the Nonneutral Sensitivity Equation

Continuing the sensitivity analysis on (4.4) requires evaluating the partial derivatives $\partial\zeta/\partial u_*$, $\partial\zeta/\partial t_*$, $\partial\zeta/\partial q_*$, $\partial\epsilon/\partial u_*$, $\partial\epsilon/\partial z$, and $\partial\epsilon/\partial\zeta$. Several of these derive easily from (1.4), which can also be written as the sum of terms due to the sensible (ζ_T) and latent (ζ_Q) heat fluxes (Busch 1973; Andreas 1989):

$$\zeta = \zeta_T + \zeta_Q = \zeta_T\left(1 + \frac{0.61T}{\rho + 0.61Q}\frac{1}{K\mathrm{Bo}}\right). \quad \text{(A.1)}$$

Here, Bo is the Bowen ratio,

$$\mathrm{Bo} = \frac{-\rho c_p u_* t_*}{-L_v u_* q_*} = \frac{t_*}{Kq_*}, \quad \text{(A.2)}$$

and K is a constant for a given set of meteorological conditions. From (1.4) and (A.1), we quickly evaluate

$$\frac{\partial\zeta}{\partial u_*} = -\frac{2\zeta}{u_*}, \quad \text{(A.3)}$$

$$\frac{\partial\zeta}{\partial z} = \frac{\zeta}{z}, \quad \text{(A.4)}$$

$$\frac{\partial\zeta}{\partial t_*} = \frac{\zeta_T}{t_*}, \quad \text{(A.5)}$$

$$\frac{\partial\zeta}{\partial q_*} = \frac{\zeta_Q}{q_*}. \quad \text{(A.6)}$$

From (1.3),

$$\frac{\partial\epsilon}{\partial u_*} = \frac{3u_*^2}{kz}\phi_\epsilon(\zeta) + \frac{u_*^2}{zk}\frac{\partial\zeta}{\partial u_*}\frac{\partial\phi_\epsilon}{\partial\zeta}. \quad \text{(A.7)}$$

With (A.3), this becomes

$$\frac{\partial\epsilon}{\partial u_*} = \frac{\epsilon}{u_*}\left(3 - \frac{2\zeta}{\phi_\epsilon}\frac{\partial\phi_\epsilon}{\partial\zeta}\right), \quad \text{(A.8)}$$

where, from (4.1),

$$\frac{\zeta}{\phi_\epsilon}\frac{\partial\phi_\epsilon}{\partial\zeta} = \frac{0.46(-\zeta)^{2/3}}{1+0.46(-\zeta)^{2/3}} \quad \text{for} \quad -10 \leq \zeta \leq 0, \tag{A.9a}$$

$$= \frac{(0.9)(2.3)\zeta^{3/5}}{1+2.3\zeta^{3/5}} \quad \text{for} \quad 0 \leq \zeta \leq 2. \tag{A.9b}$$

Next, consider $\partial\epsilon/\partial z$. From (1.3), this is

$$\frac{\partial\epsilon}{\partial z} = -\frac{u_*^2}{kz^2}\phi_\epsilon + \frac{u_*^2}{kz}\frac{\partial\zeta}{\partial z}\frac{\partial\phi_\epsilon}{\partial\zeta}. \tag{A.10}$$

With (A.4), this becomes

$$\frac{\partial\epsilon}{\partial z} = -\frac{\epsilon}{z}\left(1-\frac{\zeta}{\phi_\epsilon}\frac{\partial\phi_\epsilon}{\partial\zeta}\right). \tag{A.11}$$

Also from (1.3),

$$\frac{\partial\epsilon}{\partial\zeta} = \frac{u_*^3}{kz}\frac{\partial\phi_\epsilon}{\partial\zeta} = \frac{\epsilon}{\zeta}\left(\frac{\zeta}{\phi_\epsilon}\frac{\partial\phi_\epsilon}{\partial\zeta}\right). \tag{A.12}$$

On substituting (A.3)–(A.6), (A.8), (A.11), and (A.12) into (4.4), we get

$$\frac{d\epsilon}{\epsilon} = \left[3-4\left(\frac{\zeta}{\phi_\epsilon}\frac{\partial\phi_\epsilon}{\partial\zeta}\right)\right]\frac{du_*}{u_*} + \left[-1+2\left(\frac{\zeta}{\phi_\epsilon}\frac{\partial\phi_\epsilon}{\partial\zeta}\right)\right]\frac{dz}{z} + \left(\frac{\zeta}{\phi_\epsilon}\frac{\partial\phi_\epsilon}{\partial\zeta}\right)\left(\frac{\zeta_T}{\zeta}\frac{dt_*}{t_*} + \frac{\zeta_Q}{\zeta}\frac{dq_*}{q_*}\right). \tag{A.13}$$

This is quite an important intermediate result. It shows how precisely we can estimate ϵ from any values of u_*, t_*, q_*, and z at our disposal. For example, u_*, t_*, and q_* could have come from eddy-correlation measurements such as those implied by (1.5)–(1.7). Alternatively, we could solve (A.13) for du_*/u_*. The result would then be a sensitivity equation that predicts how precisely we could measure u_* using the dissipation method (Fairall and Larsen 1986). Although variations on the dissipation method have been used since Taylor (1961) formulated the method in 1961, this is the first sensitivity analysis for it that I have seen reported.

Key results in the paper by Andreas (1989) were sensitivity equations for the t_* and q_* values obtained from the λ_1 and λ_2 scintillometer measurements depicted in Fig. 1. These sensitivity equations are

$$\frac{dt_*}{t_*} = S_z\frac{dz}{z} + S_{u_*}\frac{du_*}{u_*} + S_{t_1}\frac{dC_{n1}}{C_{n1}} + S_{t_2}\frac{dC_{n2}}{C_{n2}}, \tag{A.14}$$

$$\frac{dq_*}{q_*} = S_z\frac{dz}{z} + S_{u_*}\frac{du_*}{u_*} + S_{q_1}\frac{dC_{n1}}{C_{n1}} + S_{q_2}\frac{dC_{n2}}{C_{n2}}, \tag{A.15}$$

where the S's here are sensitivity coefficients appropriate to that problem, and C_{n1} and C_{n2} are the square roots of the refractive index structure parameters measured by the λ_1 and λ_2 scintillometers (i.e., C_{n1}^2 and C_{n2}^2). Andreas gave the functional forms for the S's and showed plots of them. Here S_z and S_{u_*} depend only on ζ; S_{t_1}, S_{t_2}, S_{q_1}, and S_{q_2} depend on ζ, on the Bowen ratio, and on the two scintillometer wavelengths.

Equations (A.14) and (A.15) substitute directly into (A.13). We derive

$$\left[1+\frac{1}{3}\left(\frac{\zeta}{\phi_\epsilon}\frac{\partial\phi_\epsilon}{\partial\zeta}\right)(S_{u_*}-4)\right]\frac{du_*}{u_*} = \frac{1}{3}\frac{d\epsilon}{\epsilon} + \frac{1}{3}\left[1-\left(\frac{\zeta}{\phi_\epsilon}\frac{\partial\phi_\epsilon}{\partial\zeta}\right)(S_z+2)\right]\frac{dz}{z} - \frac{1}{3}\left(\frac{\zeta}{\phi_\epsilon}\frac{\partial\phi_\epsilon}{\partial\zeta}\right)\left(\frac{\zeta_T}{\zeta}S_{t_1} + \frac{\zeta_Q}{\zeta}S_{q_1}\right)\frac{dC_{n1}}{C_{n1}} - \frac{1}{3}\left(\frac{\zeta}{\phi_\epsilon}\frac{\partial\phi_\epsilon}{\partial\zeta}\right)\left(\frac{\zeta_T}{\zeta}S_{t_2} + \frac{\zeta_Q}{\zeta}S_{q_2}\right)\frac{dC_{n2}}{C_{n2}}. \tag{A.16}$$

On defining

$$f(\zeta) \equiv \left[1+\frac{1}{3}\left(\frac{\zeta}{\phi_\epsilon}\frac{\partial\phi_\epsilon}{\partial\zeta}\right)(S_{u_*}-4)\right]^{-1}, \tag{A.17}$$

we finally derive an equation that predicts the uncertainty in u_* that is a consequence of uncertainties in the fundamental observables ϵ (or l_0), z, C_{n1}^2, and C_{n2}^2;

$$\frac{du_*}{u_*} = S_\epsilon\frac{d\epsilon}{\epsilon} + S_{zz}\frac{dz}{z} + S_{C_1}\frac{dC_{n1}}{C_{n1}} + S_{C_2}\frac{dC_{n2}}{C_{n2}}, \tag{A.18}$$

where

$$S_\epsilon = \frac{1}{3}f(\zeta), \tag{A.19}$$

$$S_{zz} = \frac{1}{3}f(\zeta)\left[1-\left(\frac{\zeta}{\phi_\epsilon}\frac{\partial\phi_\epsilon}{\partial\zeta}\right)(S_z+2)\right], \tag{A.20}$$

$$S_{C_1} = -\frac{1}{3}f(\zeta)\left(\frac{\zeta}{\phi_\epsilon}\frac{\partial\phi_\epsilon}{\partial\zeta}\right)\left(\frac{\zeta_T}{\zeta}S_{t_1} + \frac{\zeta_Q}{\zeta}S_{q_1}\right), \tag{A.21}$$

$$S_{C_2} = -\frac{1}{3}f(\zeta)\left(\frac{\zeta}{\phi_\epsilon}\frac{\partial\phi_\epsilon}{\partial\zeta}\right)\left(\frac{\zeta_T}{\zeta}S_{t_2} + \frac{\zeta_Q}{\zeta}S_{q_2}\right). \tag{A.22}$$

REFERENCES

Andreas, E. L., 1987: On the Kolmogorov constants for the temperature–humidity cospectrum and the refractive index spectrum. *J. Atmos. Sci.*, **44**, 2399–2406.

——, 1988a: Estimating averaging times for point and path-averaged measurements of turbulence spectra. *J. Appl. Meteor.*, **27**, 295–304.

——, 1988b: Estimating C_n^2 over snow and sea ice from meteorological data. *J. Opt. Soc. Amer. A*, **5**, 481–495.

——, 1989: Two-wavelength method of measuring path-averaged turbulent surface heat fluxes. *J. Atmos. Oceanic Technol.*, **6**, 280–292.

——, 1990a: Path-averaged turbulent heat fluxes from scintillation measurements at two wavelengths. *Propagation Engineering: Third in a Series, Proc. SPIE,* **1312,** L. R. Bissonnette and W. B. Miller, Eds., Society of Photo-Optical Instrumentation Engineers, 93–105.

——, 1990b: Three-wavelength method of measuring path-averaged turbulent heat fluxes. *J. Atmos. Oceanic Technol.,* **7,** 801–814.

——, 1991: Using scintillation at two wavelengths to measure path-averaged heat fluxes in free convection. *Bound.-Layer Meteor.,* **54,** 167–182.

Azoulay, E., V. Thiermann, A. Jetter, A. Kohnle, and Z. Azar, 1988: Optical measurements of the inner scale of turbulence. *J. Phys. D: Appl. Phys.,* **21,** S41–S44.

Ben-Yosef, N., E. Goldner, and A. Weitz, 1986: Two-color correlation of scintillations. *Appl. Opt.,* **25,** 3486–3489.

Busch, N. E., 1973: On the mechanics of atmospheric turbulence. *Workshop on Micrometeorology,* D. A. Haugen, Ed., Amer. Meteor. Soc., 1–65.

Fairall, C. W., and S. E. Larsen, 1986: Inertial-dissipation methods and turbulent fluxes at the air–ocean interface. *Bound.-Layer Meteor.,* **34,** 287–301.

——, R. Markson, G. E. Schacher, and K. L. Davidson, 1980: An aircraft study of turbulence dissipation rate and temperature structure function in the unstable marine atmospheric boundary layer. *Bound.-Layer Meteor.,* **19,** 453–469.

Frehlich, R. G., 1988: Estimation of the parameters of the atmospheric turbulence spectrum using measurements of the spatial intensity covariance. *Appl. Opt.,* **27,** 2194–2198.

Gray, D. A., and A. T. Waterman, Jr., 1970: Measurement of fine-scale atmospheric structure using an optical propagation technique. *J. Geophys. Res.,* **75,** 1077–1083.

Haugen, D. A., J. C. Kaimal, and E. F. Bradley, 1971: An experimental study of Reynolds stress and heat flux in the atmospheric surface layer. *Quart. J. Roy. Meteor. Soc.,* **97,** 168–180.

Hill, R. J., 1982: Theory of measuring the path-averaged inner scale of turbulence by spatial filtering of optical scintillation. *Appl. Opt.,* **21,** 1201–1211.

——, 1988: Comparison of scintillation methods for measuring the inner scale of turbulence. *Appl. Opt.,* **27,** 2187–2193.

——, and S. F. Clifford, 1978: Modified spectrum of atmospheric temperature fluctuations and its application to optical propagation. *J. Opt. Soc. Am.,* **68,** 892–899.

——, and G. R. Ochs, 1978: Fine calibration of large-aperture optical scintillometers and an optical estimate of inner scale of turbulence. *Appl. Opt.,* **17,** 3608–3612.

——, and ——, 1983: Surface-layer micrometeorology by optical scintillation techniques. *Remote Probing of the Atmosphere,* Technical Digest of the Topical Meeting on Optical Techniques for Remote Probing of the Atmosphere, Incline Village, Nevada, Opt. Soc. Amer., TuC16.1–TuC16.4.

——, and R. J. Lataitis, 1989: Effect of refractive dispersion on the bichromatic correlation of irradiances for atmospheric scintillation. *Appl. Opt.,* **28,** 4121–4125.

——, R. A. Bohlander, S. F. Clifford, R. W. McMillan, J. T. Priestley, and W. P. Schoenfeld, 1988: Turbulence-induced millimeter-wave scintillation compared with micrometeorological measurements. *IEEE Trans. Geosci. Remote Sensing,* **26,** 330–342.

——, G. R. Ochs, and J. J. Wilson, 1992: Measuring surface-layer fluxes of heat and momentum using optical scintillation. *Bound.-Layer Meteor.,* **58,** 391–408.

Ishimaru, A., 1978: *Wave Propagation and Scattering in Random Media, Volume 2, Multiple Scattering, Turbulence, Rough Surfaces, and Remote Sensing.* Academic Press, 572 pp.

Kohsiek, W., and M. H. A. J. Herben, 1983: Evaporation derived from optical and radio-wave scintillation. *Appl. Opt.,* **22,** 2566–2570.

Livingston, P. M., 1972: Proposed method of inner scale measurement in a turbulent atmosphere. *Appl. Opt.,* **11,** 684–687.

Moroni, C., A. Navarra, and R. Guzzi, 1990: Estimation of the turbulent fluxes in the surface layer using the inertial dissipation method: A Monte Carlo error analysis. *Bound.-Layer Meteor.,* **50,** 339–354.

Ochs, G. R., and R. J. Hill, 1985: Optical-scintillation method of measuring turbulence inner scale. *Appl. Opt.,* **24,** 2430–2432.

Schacher, G. E., K. L. Davidson, T. Houlihan, and C. W. Fairall, 1981: Measurements of the rate of dissipation of turbulent kinetic energy, ϵ, over the ocean. *Bound.-Layer Meteor.,* **20,** 321–330.

Strohbehn, J. W., 1970: The feasibility of laser experiments for measuring the permittivity spectrum of the turbulent atmosphere. *J. Geophys. Res.,* **75,** 1067–1076.

Tatarski, V. I., 1961: *Wave Propagation in a Turbulent Medium.* Dover, 285 pp.

Taylor, R. J., 1961: A new approach to the measurement of turbulent fluxes in the lower atmosphere. *J. Fluid Mech.,* **10,** 449–458.

Tennekes, H., and J. L. Lumley, 1972: *A First Course in Turbulence.* MIT Press, 300 pp.

Thiermann, V., and E. Azoulay, 1989: Modeling of structure constant and inner scale of refractive index fluctuations—An experimental investigation. *Propagation Engineering, Proc. SPIE,* **1115,** N. S. Kopieka and W. B. Miller, Eds., Society of Photo-Optical Instrumentation Engineers, 124–135.

——, and H. Grassl, 1992: The measurement of turbulent surface layer fluxes by use of bichromatic scintillation. *Bound.-Layer Meteor.,* **58,** 367–389.

Wang, T. I., G. R. Ochs, and S. F. Clifford, 1978: A saturation-resistant optical scintillometer to measure C_n^2. *J. Opt. Soc. Amer.,* **68,** 334–338.

Wyngaard, J. C., 1973: On surface-layer turbulence. *Workshop on Micrometeorology,* D. A. Haugen, Ed., Amer. Meteor. Soc., 101–149.

——, and O. R. Côté, 1971: The budgets of turbulent kinetic energy and temperature variance in the atmospheric surface layer. *J. Atmos. Sci.,* **28,** 190–201.

——, and S. F. Clifford, 1978: Estimating momentum, heat and moisture fluxes from structure parameters. *J. Atmos. Sci.,* **35,** 1204–1211.